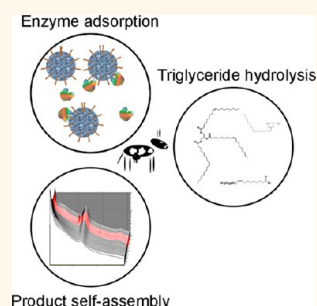


Formation of Highly Organized Nanostructures during the Digestion of Milk

Stefan Salentinig,^{†,*} Stephanie Phan,[†] Jamal Khan,[†] Adrian Hawley,[‡] and Ben J. Boyd^{†,*}

[†]Drug Delivery, Disposition and Dynamics, Monash Institute of Pharmaceutical Sciences, Monash University (Parkville Campus), 381 Royal Parade, Parkville, Victoria 3052, Australia and [‡]SAXS/WAXS beamline, Australian Synchrotron, 800 Blackburn Road, Clayton, Victoria 3168, Australia

ABSTRACT Nature's own emulsion, milk, consists of nutrients such as proteins, vitamins, salts, and milk fat with primarily triglycerides. The digestion of milk fats is the key to the survival of mammal species, yet it is surprising how little we understand this process. The lipase-catalyzed hydrolysis of dietary fats into fatty acids and monoglyceride is essential for efficient absorption of the fat by the enterocytes. Here we report the discovery of highly ordered geometric nanostructures during the digestion of dairy milk. Transitions from normal emulsion through a variety of differently ordered nanostructures were observed using time-resolved small-angle X-ray scattering on a high-intensity synchrotron source and visualized by cryogenic transmission electron microscopy. Water and hydrophilic molecules are transferred into the lipid phase of the milk particle, turning the lipid core gradually into a more hydrophilic environment. The formation of highly ordered lipid particles with substantial internal surface area, particularly in low-bile conditions, may indicate a compensating mechanism for maintenance of lipid absorption under compromised lipolysis conditions.



KEYWORDS: self-assembly · hierarchically organized emulsions · liquid crystalline structures · vesicles · morphological transition · digestion of lipid · milk

Milk is the major source of nutrients in early life and key to the survival of mammal species. It is also a highly valuable food product in the Western diet.^{1,2} Milk is a natural protein-stabilized emulsion containing water- and oil-soluble vitamins, salts, proteins, carbohydrates, milk fat, and a variety of other hydrophobic bioactive components.^{1–4} The oil-soluble components are dispersed in micrometer-sized emulsion particles in the aqueous host media. The total water content in milk is approximately 87% (w/w), while triglycerides consisting mainly of palmitic (C₁₆) and oleic (C_{18:1}) acids form the major oil component in full cream milk.^{5,6} Among further lipids and hydrophobic constituents in milk are lipid-soluble vitamins (A, D, E, K), cholesterol and cholesterol esters, phospholipids, and fatty acids.⁷ Dairy milk lipids are also the major component of many daily food products such as cheese, milk, ice-cream, and yogurt.

In this report we present the self-assembly of dairy milk components to form nanostructures during their *in vitro* digestion under simulated *in vivo* conditions of the gastrointestinal tract. There the milk ingredients

are transformed to smaller molecular weight, more hydrophilic components by different digestive enzymes to enable absorption.⁸ The water-soluble lipase anchors at the milk emulsion–droplet interface to hydrolyze the sn1 and sn3 position of the dietary triglyceride fats to form an sn2 monoglyceride and two fatty acids. This reaction plays a vital role in the delivery of the lipid-soluble bioactive molecules contained in the milk to the circulatory system of the body.^{9–14} It is a complex process involving a variety of amphiphilic molecules and different pH, osmotic, and mechanical shear conditions.^{15–17} The digestion of the lipids in the small intestine is promoted by secretion of sodium bicarbonate, which neutralizes the food bolus, leading to a pH between 6.0 and 6.6. This is close to the optimum pH for the activity of the pancreatic lipase at pH = 6.5.^{16,17} Gall bladder contraction leads to secretion of biliary juice containing mainly phospholipids, cholesterol, and bile salts.^{16,19–23} These help to stabilize the emulsion in the digestive juice and further modify the oil/water interface for the adsorption of the lipase–colipase complex catalyzing the reaction.^{18,19} It has been shown that

* Address correspondence to ben.boyd@monash.edu; stefan.salentinig@gmail.com.

Received for review August 22, 2013 and accepted November 6, 2013.

Published online November 06, 2013 10.1021/nn405123j

© 2013 American Chemical Society

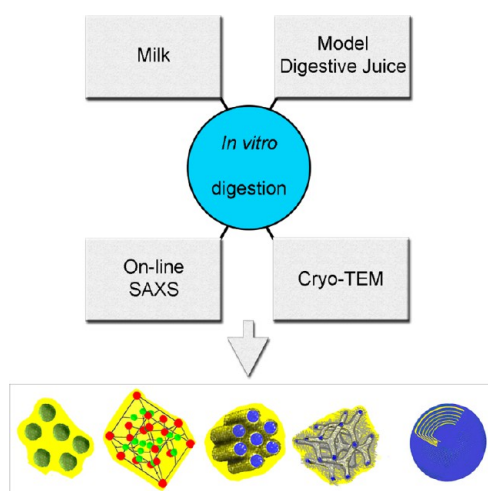


Figure 1. Schematic illustration of the *in vitro* digestion of milk using time-resolved SAXS and cryo-TEM. The reaction kinetics of the biological process of milk digestion is studied by the detection of product and colloidal structure formation and transformation with time of digestion. The schematics of the observed oil-continuous structures are microemulsion, micellar cubic, hexagonal, and bicontinuous cubic phase, and multilamellar vesicles, starting from left.

the emulsion particle size influences the kinetics of lipid digestion; smaller emulsion particles provide a larger oil–water interfacial area to which the lipase may adsorb, leading to faster digestion, which influences the rate of change in composition of the system.²⁴

The amphiphilic digestion products of the milk triglycerides, namely, monoglyceride and fatty acid, when combined in certain ratios are known to self-assemble in water to form a wide variety of structures including those illustrated in Figure 1. This includes the lamellar phase, the inverted type hexagonal phase (H_2), the bicontinuous cubic phases ($Pn3m$ and $Im3m$ type), and the inverse micellar systems such as the discontinuous cubic phase ($Fd3m$) and inverse micelles (L_2).^{25–27} The self-assembled structures that form in these systems depend on the molecular geometry of the amphiphilic lipids, the composition, and environmental factors such as salt concentration and pH, and can be described by the critical packing parameter model.²⁸ Mixed micelles and vesicles formed by monoglycerides, fatty acids, and bile salts have been proposed as the self-assembled systems responsible for the transport of the hydrophobic food components. They carry food through the unstirred water layer to the brush border membrane of the enterocytes, the absorptive cells in the small intestine.^{29–31} However, it is not yet clear whether structures formed under equilibrium “assembled” conditions have relevance to the non-equilibrium, dynamic conditions prevalent during digestion *in vivo*.

To this end, there have been recent attempts to probe self-assembly structure using time-resolved scattering approaches under digestive conditions.

The digestion of model emulsion systems containing triolein, tricaprylin, and other pharmaceutically relevant lipids has revealed the formation of hierarchically organized emulsions containing the aforementioned liquid crystalline phases.^{14,32,33} However, to our knowledge, no such studies have been performed on more complex nutritionally relevant substrates such as milk.

Here the real-time formation of hierarchically organized emulsions containing highly ordered self-assembled nanostructures during digestion of dairy bovine milk under physiologically relevant conditions is reported. The low volume fraction of milk fat in the model digestive juice and anticipated fast kinetics of transformations in colloidal structure were challenges to be overcome. Thus, a high-intensity synchrotron radiation source was necessary for *in situ* time-resolved scattering experiments with sub-minute resolution. Hence a highly contemporary approach coupling time-resolved small-angle X-ray scattering (SAXS) on a high-intensity synchrotron source with cryogenic transmission electron microscopy (cryo-TEM) for the detection and confirmation of the self-assembled structures with nanometer-scale resolution during the *in vitro* digestion of milk is achieved. The effect of bile concentration on kinetics and structure formation is elucidated and related to possible implications for nutrition in bile-compromised individuals.

RESULTS AND DISCUSSION

The digestion of milk, a common biological system essential to life, is a process involving concepts from chemistry, physics, material science, and biology. Digestion of lipids by lipases has been previously studied using microscopy techniques.^{44,45} While textures can be observed at the surface of the digesting oil droplets, clear structure assignment is not possible. The unambiguous assignment of structures and detection of lesser populations in mixed phase systems require the specificity of scattering approaches such as those presented in the current study on milk. During the *in situ* SAXS measurements the digestion reaction was monitored by the detection of fatty acids (see Supporting Information, Figure SI-1). This information is used to correlate the colloidal structures to the sample composition. Approximately 50% digestion was achieved after 1 min, and saturation was reached after less than 30 min, independent of the total bile salt concentration. In the absence of pancreatin, no free fatty acid formation or transformation in colloidal structure was observed, as the lipase is a prerequisite for the digestion to occur (see Supporting Information, SI-2).

Digestion in the Absence of Bile Components. The SAXS data for the lipase-catalyzed digestion of milk in the absence of bile salts are presented in Figure 2. Over time there was significant ordering of the molecules to form self-assembled structures within the oil droplets under action of the enzyme. Prior to digestion, milk is a

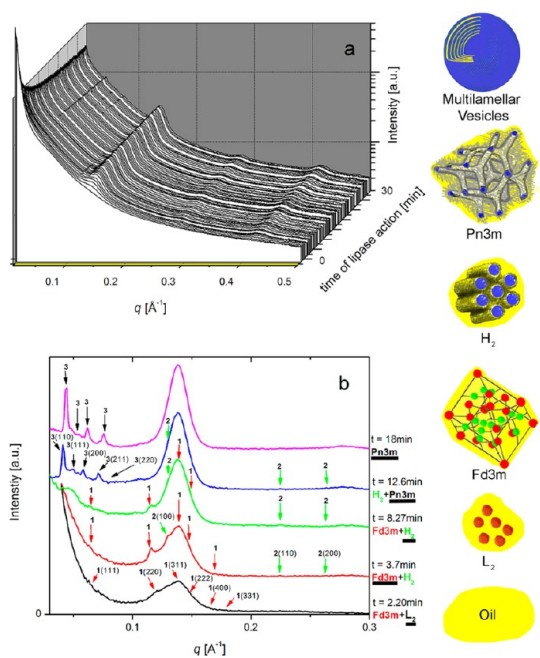


Figure 2. SAXS profiles for the digestion of milk in the absence of bile salt over 30 min at $T = 37\text{ }^{\circ}\text{C}$ and $\text{pH} = 6.5$ at $\text{TG}/\text{pancreatin} = 0.075$: (a) transition of structures with time of lipase action on milk and (b) SAXS profiles at selected time points after baseline subtraction. The identifiable Bragg peaks and further calculated theoretical peak positions are indexed with the corresponding Miller indices and labeled 1, 2, and 3 for $Fd3m$, H_2 , and $Pn3m$ structures, respectively. Schematics of the structures are presented according to their appearance.

normal unstructured oil-in-water emulsion ($t = 0$ in Figure 2a). The scattering curves represent milk in buffer at $\text{pH} = 6.5$ and $T = 37\text{ }^{\circ}\text{C}$. The shape of the SAXS scattering curves indicates the presence of proteins and protein aggregates as well the low- q upturn due to the scattering of the large emulsion particles with a defined volume. Addition of pancreatin leads to the digestion of the milk triglycerides: Partial digestion of the triglyceride (up to 50% from SI-1) to produce mainly diglycerides and fatty acids renders the system more hydrophilic. After less than 1 min of lipase action a broad correlation peak formed with a maximum at approximately $q = 0.138\text{ }^{\circ}\text{Å}^{-1}$, indicating the formation of inverse, oil-continuous micelles inside the emulsion droplet (emulsified microemulsion (EME) or emulsified L_2 phase). The resulting droplets are hierarchically organized containing the thermodynamically stable oil-continuous phase inside the kinetically stabilized emulsion particle. In addition, higher order reflections at $q = 0.267$ and $0.412\text{ }^{\circ}\text{Å}^{-1}$ appeared. Together with the EME peak at $q = 0.138\text{ }^{\circ}\text{Å}^{-1}$ the three equidistant peaks result from the scattering of a lamellar phase with the calculated lattice constant of $45\text{ }^{\circ}\text{Å}$ (separation distance of the bilayers). An increase in the intensity of the equidistant peaks for the lamellar structure but no discernible change in peak positions was observed.

Further digestion ($>60\%$ from SI-1) increases the population of these structures with packing into an ordered $Fd3m$ lattice required to accommodate the increased proportion and hydrophilicity of the amphiphilic constituents and concomitant water: As highlighted in Figure 2 b, after 2 min of digestion further Bragg peaks formed near the broad EME peak. These peak positions (at $q = 0.119$, 0.141 , and $0.146\text{ }^{\circ}\text{Å}^{-1}$) correspond to reflections from the $Fd3m$ -type micellar cubic structure with a lattice constant of around $150\text{ }^{\circ}\text{Å}$ (distance between the micelles arranged on a cubic lattice).

Bragg peaks of the inverse hexagonal phase at $q = 0.130$, 0.224 , and $0.259\text{ }^{\circ}\text{Å}^{-1}$ with a lattice constant of $56\text{ }^{\circ}\text{Å}$ develop after 2.5 min (around 70% digested triglyceride; see SI-1). These reflections became more defined and grew over time before vanishing after approximately 15 min of digestion time.

At approximately $t = 10$ min ($\sim 90\%$ of triglycerides digested, from SI-1) further reflections appeared at $q = 0.041$, 0.050 , 0.058 , and $0.071\text{ }^{\circ}\text{Å}^{-1}$ from the bicontinuous cubic $Pn3m$ structure with a lattice constant of $217\text{ }^{\circ}\text{Å}$. This results in the need to incorporate a much greater proportion of water, likely in the vicinity of 40% w/w, which is required to form the bicontinuous cubic structure. Consequently, the water content increases from close to 0% for the triglyceride oil before digestion to $>33\%$ for the bicontinuous cubic phase toward the end of the digestion process.^{36–38} In these structures, water is confined into nanometer-scale cavities, forming layers with molecular organization different from that of bulk water.^{39–41} So-called nanoscopic masks of organized water near interfaces with different polarity have also been discussed to influence the hydrophobic effect.⁴¹ Self-assembly as well as the interaction between proteins with the colloidal structures and their hydrophobic substrates could be modified by the presence and change in the subaqueous water layer in biological systems, which needs further investigation in the context of lipid digestion. The exchange of bulk water with the aqueous phase also induces the transfer of amphiphilic and hydrophilic food components (e.g., carbohydrates, proteins) into the interior structure of the emulsion. The $Pn3m$ structure remained present through to completion of digestion with small changes in the lattice constant to $200\text{ }^{\circ}\text{Å}$ within 20 min of appearance of the cubic structure.

The sequence of phases observed during digestion in the absence of bile (oil \rightarrow EME \rightarrow $Fd3m$ cubic \rightarrow inverse hexagonal \rightarrow bicontinuous cubic) is in line with expectation on consideration of the packing parameter in such systems. Such a progression has been observed in equilibrium systems on addition of cubic phase forming lipids such as phytantriol, monoolein, and monolinolein to hydrocarbons and triglycerides.^{36,42,43} Generation of structures is typically achieved by careful selection of lipid composition^{25,36,37} or less

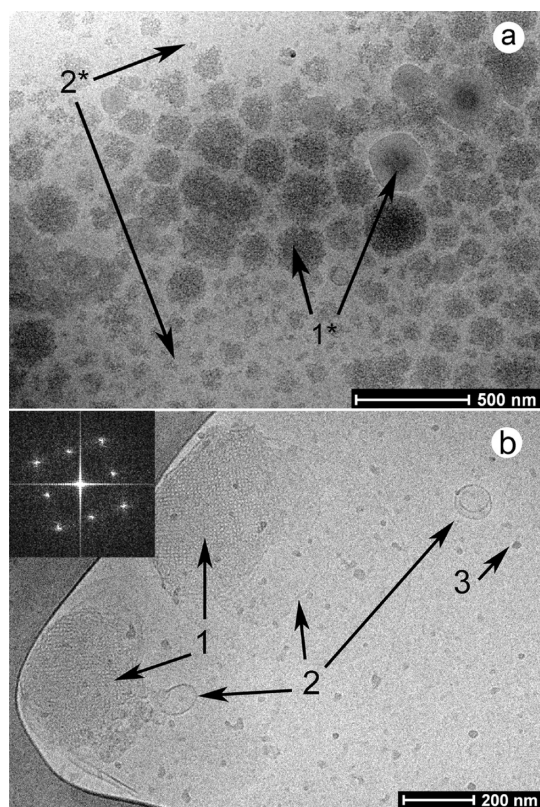


Figure 3. Cryo-TEM images of samples taken (a) before and (b) after the digestion of milk for the sample for which the scattering is shown in Figure 2. Before lipase addition emulsion droplets (labeled as 1*) and milk protein micelles of varying size (2*) are the dominant structures. After digestion internally structured emulsion particles containing bicontinuous cubic phase (1) with vesicles separating from their surface (2) and protein particles (3) are present. The large continuous dark areas in the images represent the carbon film supporting the amorphous ice layer. The inset shows the Fourier transform of the magnified cubic phase area.

commonly through changes in pH^{26,49} or the presence of certain ions^{52,53} to modulate the packing parameter of the lipids. These highly ordered structures have been of interest recently in the pharmaceutical delivery field. This is due to the capacity to tune the controlled release of active molecules through control of internal nanostructure.^{46–51} Using enzymatic processes to deliberately generate such structures for functional purposes in a complex nutritionally relevant substrate is clearly indicated by the results of this study and has not been reported previously.

The corresponding cryo-TEM images visualizing the structures formed during digestion of milk in the absence of bile components are presented in Figure 3a and b. The cryo-TEM images supported the presence of a cubic phase evident from the scattering measurements, but indicated a complex mixture of particles as expected. Prior to addition of pancreatin, protein-stabilized emulsion droplets up to 600 nm in diameter and milk protein micelles of varying size were observed. After digestion, internally structured emulsion particles with a particle mean diameter of

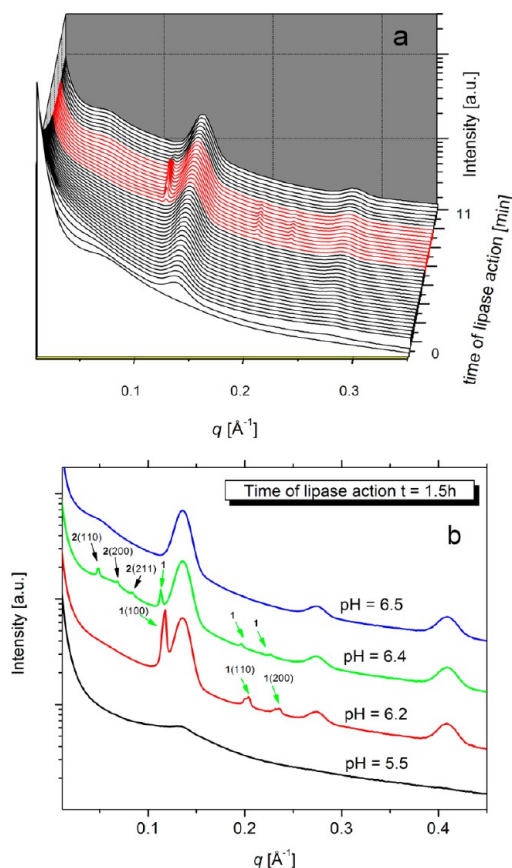


Figure 4. SAXS profiles acquired during the digestion of milk in the presence of bile salt at $T = 37\text{ }^{\circ}\text{C}$ at TG/BS = 33.6 and TG/pancreatin = 0.175: (a) online measurements during milk digestion at pH = 6.5 showing the transition of structures with time of lipase action; (b) effect of pH variation on the structures formed evident from the changes in SAXS profiles at the end of the digestion process. The identifiable Bragg peaks and further calculated theoretical peak positions are indexed with the corresponding Miller indices and labeled as 1 and 2 for H_2 and $Im3m$, respectively. The corresponding cryo-TEM images visualizing the colloidal structures in these samples are presented in Figure 5.

several hundred nanometers possessing the bicontinuous cubic phase structure, in coexistence with anisotropic structures, were apparent. The Fourier transform of the structured areas shows periodic ordering with a 45° angle between reflections as expected for a cubic-type lattice.⁵⁴ Large vesicles were also present at the particle surface. In addition, uni- and multilamellar liposomes, tubular structures, and multilamellar fragments transitioning to cubosomes can be observed. Long strands of collagen, several micrometers in length and 100 nm in width, originating from the pancreatin extract were also present (see Supporting Information, SI-3).

The observation that reduced (or zero) concentration of bile salt present during digestion promoted the formation of the nonlamellar liquid crystalline structures, such as the cubic phase, with high internal surface area may have relevance in facilitating digestion of lipids in bile-compromised individuals.

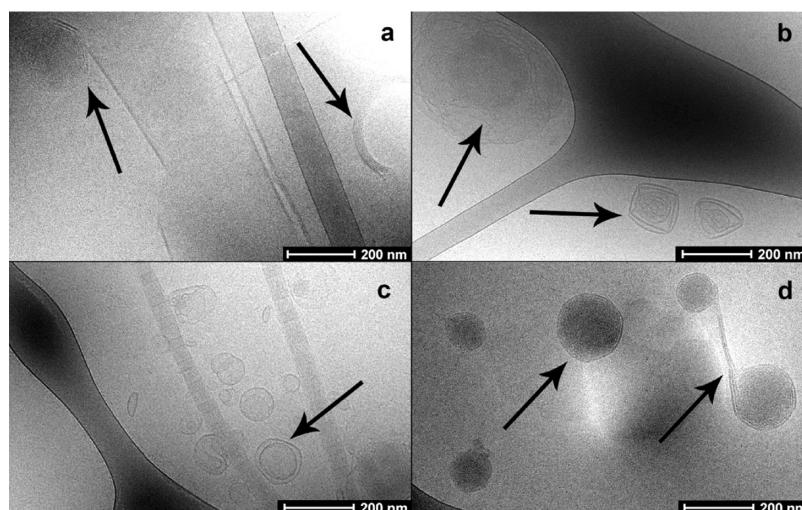


Figure 5. Cryo-TEM pictures during the digestion of milk under the conditions presented in Figure 4. (a) After 7 min of digestion, tubular structures, multilamellar aggregates, and emulsion particles transferring to hexagonally structured aggregates can be observed. (b) After 11 min of digestion, vesicles and vesicular structures developing on the surface of cubosomes can be seen. (c) After 30 min of digestion, vesicles of different size and shape are the dominating structures. (d) After 30 min at pH = 6.4, hexagonally structured particles, some of them interconnected, are present.

Digestion in the Presence of Bile Components. Bile salt forms micelles at the concentrations used in this study. The control experiments showing the scattering profiles of the bile salt micelles and the bile salt–pancreatin mixture, indicating the presence of proteins and protein aggregates in combination with the micelles, are presented in the Supporting Information, SI-2a.

The addition of the bile salt mixture to milk resulted in a SAXS pattern representing milk components in combination with the bile salt micelles. Before lipase addition, the scattering was constant over minutes and no fatty acid formation was observed (see Supporting Information, SI-2b). The digestion of milk started immediately after pancreatin addition. The scattering curves for the digestion in the presence of pancreatin at low bile salt concentration (TG/BS = 33.6 and TG/pancreatin = 0.175) are presented in Figure 4. The transition from emulsion to emulsified microemulsion occurred after less than 1 min (about 50% digestion of the triglycerides), indicated by the formation of the broad EME peak at $q = 0.135 \text{ \AA}^{-1}$. The Bragg peaks at $q = 0.137, 0.275,$ and 0.408 \AA^{-1} for the lamellar structure with a lattice constant of 46 \AA were observed during the full time of digestion. In addition, the transient presence of hexagonal structure is indicated after 6 min of digestion by the formation of Bragg peaks at $q = 0.118, 0.204,$ and 0.236 \AA^{-1} with a lattice constant of 64 \AA . The hexagonal structure diminished after 9 min of lipase action, and a broad peak developed between $q = 0.04$ and 0.08 \AA^{-1} and remained until the end of the digestion experiment (90 min).

Time-resolved cryo-TEM images in Figure 5 confirm the results obtained from SAXS. The images taken after 7 min show tubular structures, multilamellar aggregates, and emulsion particles transferring to hexagonally

structured particles. After 11 min of digestion vesicular structures developed on the surface of cubosomes, and after 30 min vesicles of different size and shape were the dominating structures.

Changes in the lattice parameter and phase structure with bile salt concentration measured with SAXS showed that bile salt is incorporated into the self-assembled structure inside the emulsion particle. Increasing bile salt concentration gradually leads to more hydrophilic interfaces and swelling of the internal structures. This effect is similar to a longer time of lipase action and supported by the data showing a swelling of the lamellar (lattice constant from 45 to 46 \AA) and inverse hexagonal structure (lattice constant from 56 to 64 \AA). Further increase in the bile salt concentration leads to the formation of the multilamellar vesicles dominating the scattering signal (see Supporting Information, SI-4). The cryo-TEM of digested milk at increased bile salt concentration shows the presence of multilamellar fragments up to 400 nm in length, tubular structures, and multilamellar fragments as well as unilamellar vesicles; no liquid crystalline structures of higher order were present, in agreement with the SAXS data (see Supporting Information, SI-5). From a colloidal perspective this result indicates faster digestion of the lipid in milk in the presence of bile salt.

Effect of pH on Structure Formation. The effect of changing the pH in the final digestion sample at low bile salt concentration (TG/BS = 33.6 after 90 min) is presented in Figure 4b. It resulted in substantial changes to self-assembly behavior. At pH = 6.5 the Bragg peaks for the lamellar structure and a broad peak between $q = 0.04$ and 0.08 \AA^{-1} were present. Upon decreasing the pH to 6.4, major Bragg reflections at $q = 0.049, 0.068,$

and 0.084 \AA^{-1} corresponding to the $Im3m$ -type bicontinuous cubic phase with a lattice constant of 184 \AA developed from this broad peak. In addition, the Bragg peaks for an inverse hexagonal phase with a lattice constant of 64 \AA appeared at $q = 0.113, 0.197,$ and 0.227 \AA^{-1} . The cryo-TEM image of this sample confirms the results from SAXS. It is dominated by hexagonally structured particles, some of them interconnected (see Figure 5d). A further decrease of pH to 6.2 leads to the disappearance of the bicontinuous cubic phase and to more defined reflections for the hexagonal phase. This included a shift of the peak positions toward higher q values ($0.118, 0.204, 0.235 \text{ \AA}^{-1}$), indicating a decrease in the lattice constant to 62 \AA . At pH = 5.5 only the correlation peak of an emulsified microemulsion was present. Consequently, decreasing pH leads to “back-tuning” of the morphological changes developed during the digestion. This confirms the pH value in the human intestine as an important factor influencing structure formations and transformations.

CONCLUSION

Hierarchically organized emulsion droplets containing a thermodynamically stable self-organized lipid core are generated during the digestion of dairy milk. The initial emulsion oil phase was gradually tuned toward more hydrophilic and highly organized

geometric structures with substantial surface areas during lipase action. The structures agree with anticipated behavior on the basis of critical packing parameters of amphiphilic molecules. The identification of a self-organized geometrical order inside dairy milk emulsions during their digestion offers an attractive conceptual framework to understand lipid digestion as well as revealing potential aspects of the transport of oil-soluble food components in the aqueous environment of the gut, particularly for bile-compromised individuals. Under regular digestive conditions it is accepted that the major role of bile salt is the solubilization and transport of digestion products away from the surface of the digesting oil droplet to the enterocytes for absorption to occur. In the absence or limited availability of bile salt, significantly compromised digestion is expected. For such individuals, formation of the highly porous cubic phase structures with enhanced surface area for access by lipolytic enzymes may provide a mechanism by which quantitative digestion may still occur. This may yield an alternative mechanism that compensates for the maintenance of lipid absorption and the absorption of hydrophobic food components in the absence of or at low bile salt concentrations. This assertion is supported by the effective digestion of the milk in the complete absence of bile salt in these studies.

MATERIALS AND METHODS

Materials. Tris maleate (reagent grade) and bile salt (sodium taurodeoxycholate >95%) were purchased from Sigma Aldrich (St. Louis, MO, USA). Phospholipid (dioleoylphosphatidyl choline, DOPC, >94%) was from Trapeze Associates Pty Ltd. (Clayton, Victoria, Australia), and pancreatin extract (USP grade pancreatin activity) was from Southern Biologicals (Nunawading, Victoria, Australia). Fresh milk with up to 3.5% fat content was sourced from Sungold, Warrnambool Cheese and Butter, Victoria, Australia. An average molecular weight of 723.16 g/mol for the milk triglycerides was assumed in this study according to the reported composition of bovine milk fat.⁵ Calcium chloride (>99%) was obtained from Ajax Finechem (Seven Hills, NSW, Australia) and sodium chloride (>99%) from Chem Supply (Gillman, SA, Australia). Ultrapure water ($R > 18 \text{ M}\Omega$) was used for the preparation of all samples.

Methods. *Flow-through Lipolysis Model.* *In vitro* digestion studies were performed using a previously reported flow-through setup coupled to a quartz capillary to enable time-resolved small-angle X-ray scattering for structural elucidation in real time.³² A schematic representation of the setup is presented in Figure 1. Briefly, digestions were conducted in a thermostated glass vessel at $T = 37 \text{ }^\circ\text{C}$ under constant magnetic stirring, fitted with a pH-stat auto titrator (Radiometer, Copenhagen, Denmark) to maintain the pH of the digestion medium at pH = 6.5.

The digestion medium was drawn through a 1.5 mm diameter quartz capillary mounted in the X-ray beam at a flow rate of approximately 10 mL/min to avoid beam damage, through silicone tubing (total volume $< 1 \text{ mL}$) via a peristaltic pump. A remotely operated syringe driver was installed at the beamline to deliver 1 mL of pancreatin extract into the vessel to initiate digestion during the measurements.

Simulated intestinal fluid was prepared from a stock consisting of bile salt (BS, sodium taurodeoxycholate) and phospholipid

(DOPC) concentrations at a ratio of $20 \text{ mM}:5 \text{ mM}$ in digestion buffer (50 mM Tris maleate, 5 mM $\text{CaCl}_2 \cdot 2\text{H}_2\text{O}$, 150 mM NaCl, adjusted to pH 6.5).^{30,34} Milk (5 mL) was added to the digestion buffer, fed (BS/PC = $20 \text{ mM}/5 \text{ mM}$) or fasted (BS/PC = $5 \text{ mM}/1.25 \text{ mM}$) simulated intestinal fluid (4 mL) prior to addition of pancreatin. Pancreatin (1000 TBU in 1 mL of digestion buffer) was added using a remotely activated syringe pump. The calculated mass/mass ratios in this study were $4.2 < \text{triglyceride (TG)}/\text{bile salt (BS)} < 33.6$ and $\text{TG}/\text{pancreatin} = 0.075$ and 0.175 , covering the range of biologically relevant concentrations in the fed and fasted state of the human intestine.^{30,34} Upon addition of the pancreatin, the pH-stat titrated the digestion mixture with 0.2 M NaOH in order to maintain the system at pH 6.5.

Synchrotron small-angle X-ray scattering and flow-through *in vitro* digestion SAXS measurements were performed at the SAXS/WAXS beamline at the Australian Synchrotron. An X-ray beam with a wavelength of 1.1271 \AA (11 keV) was used. A sample to detector distance of 1015 mm gave the q -range of $0.01 < q < 0.7 \text{ \AA}^{-1}$, where q is the length of the scattering vector, defined by $q = 4\pi/\lambda \sin(\theta/2)$, λ being the wavelength and θ the scattering angle. The q range calibration was made using silver behenate as standard.³⁵ The 2D SAXS patterns were acquired for 5 s with 12 s delay between frames, using a Pilatus 1M detector with an active area $169 \times 179 \text{ mm}^2$ and with a pixel size of $172 \text{ }\mu\text{m}$ integrated into the one-dimensional scattering function $I(q)$ using the in-house developed software package ScatterBrain. Hexagonal, cubic, and lamellar space groups were determined by the relative positions of the Bragg peaks in the scattering curves, which correspond to the reflections on planes defined by their (hkl) Miller indices. Microemulsions and unilamellar vesicles were characterized by their unique scattering (e.g., the broad correlation peak reflecting the mean particle-to-particle distance for micelles and the q^{-2} dependence at low q values for locally flat bilayer structures). More complete information concerning this point can be found elsewhere.¹⁴

Cryo-TEM Studies. A laboratory-built humidity-controlled vitrification system was used to prepare the samples for cryo-TEM. Humidity was kept close to 80% for all experiments, and ambient temperature was 22 °C. Copper grids (200-mesh) coated with perforated carbon film (lacey carbon film: ProSciTech, Qld, Australia) were glow discharged in nitrogen to render them hydrophilic. Aliquots (4 mL) of the sample were pipetted onto each grid prior to plunging. After 30 s adsorption time the grid was blotted manually using Whatman 541 filter paper for approximately 2 s. Blotting time was optimized for each sample. The grid was then plunged into liquid ethane cooled by liquid nitrogen. Frozen grids were stored in liquid nitrogen until required.

The samples were examined using a Gatan 626 cryoholder (Gatan, Pleasanton, CA, USA) and Tecnai 12 transmission electron microscope (FEI, Eindhoven, The Netherlands) at an operating voltage of 120 kV. The sample holder operated at -175.5 ± 1 °C. At all times low-dose procedures were followed, using an electron dose of 8–10 electrons/Å² for all imaging. Images were recorded using an FEI Eagle 4kx4k CCD camera at magnifications ranging from 15 000× to 50 000×.

Conflict of Interest: The authors declare no competing financial interest.

Acknowledgment. The studies were funded by the Australian Research Council through the Discovery Projects scheme (DP120104032). B.J.B. holds an ARC Future Fellowship. We are grateful to Lynne Waddington for the assistance with the cryo-TEM instrument. The SAXS experiments were undertaken at the SAXS/WAXS beamline at the Australian Synchrotron, Victoria, Australia.

Supporting Information Available: The Supporting Information contains the titration profiles of free fatty acids during the digestion experiment, the control experiments showing the SAXS scattering profiles of bile salt, bile salt with milk and lipase, as well as additional SAXS and cryo-TEM data, measured during milk digestion at high bile salt concentration. This material is available free of charge via the Internet at <http://pubs.acs.org>.

REFERENCES AND NOTES

- Lindquist, S.; Hernell, O. Lipid Digestion and Absorption in Early Life: An Update. *Curr. Opin. Clin. Nutr. Metab. Care* **2010**, *13*, 314–320.
- Innis, S. M. Dietary Triacylglycerol Structure and Its Role in Infant Nutrition. *Adv. Nutr.* **2011**, *2*, 275–283.
- Jensen, R. G.; Ferris, A. M.; Lammikeefe, C. J.; Henderson, R. A. Lipids of Bovine and Human Milks – A Comparison. *J. Dairy Sci.* **1990**, *73*, 223–240.
- Swaigood, H. E. Chemistry of the Caseins. In *Advanced Dairy Chemistry*; Fox, P. F., Ed.; Elsevier: London, 1993; pp 63–110.
- Christie, W. W.; Clapperton, J. L. Structures of the Triglycerides of Cows' Milk, Fortified Milks (Including Infant Formulae), and Human Milk. *Soc. Dairy Technol.* **1982**, *35*, 22–24.
- Jensen, R. G.; Newburg, D. S. Bovine Milk Lipids. In *Handbook of Milk Composition*; Jensen, R. G., Ed.; Academic Press, Inc.: New York, 1995; pp 542–573.
- Bitman, J.; Wood, D. L. Changes in Milk Phospholipids during Lactation. *Dairy Sci.* **1990**, *73*, 1208–1216.
- Hinsberger, A.; Sandhu, B. K. Digestion and Absorption. *Curr. Paediatr.* **2004**, *14*, 605–611.
- Porter, C. J. H.; Trevasakis, N. L.; Charman, W. N. Lipids and Lipid-Based Formulations: Optimizing the Oral Delivery of Lipophilic Drugs. *Nat. Rev. Drug Discovery* **2007**, *6*, 231–248.
- Lowe, M. E. Pancreatic Triglyceride Lipase and Colipase: Insights into Dietary Fat Digestion. *Gastroenterology* **1994**, *107*, 1524–1536.
- Reis, P.; Holmberg, K.; Watzke, H.; Leser, M. E.; Miller, R. Lipases at Interfaces: A Review. *Adv. Colloid Interface Sci.* **2009**, *147–148*, 237–250.
- Rich, G. T.; Fillery-Travis, A.; Parker, M. L. Low pH Enhances the Transfer of Carotene from Carrot Juice to Olive Oil. *Lipids* **1998**, *33*, 985–992.
- Wright, A. J.; Pietrangelo, C.; MacNaughton, A. Influence of Simulated Upper Intestinal Parameters on the Efficiency of Beta Carotene Micellarisation using an *in Vitro* Model of Digestion. *Food Chem.* **2008**, *107*, 1253–1260.
- Salentinig, S.; Sagalowicz, L.; Leser, M. E.; Tedeschi, C.; Glatter, O. Transitions in the Internal Structure of Lipid Droplets during Fat Digestion. *Soft Matter* **2011**, *7*, 650–661.
- Golding, M.; Wooster, T. J. The Influence of Emulsion Structure and Stability on Lipid Digestion. *Curr. Opin. Colloid Interface Sci.* **2010**, *15*, 90–101.
- Kalantzi, L.; Goumas, K.; Kalioras, V.; Abrahamsson, B.; Dressman, J.; Reppas, C. Characterization of the Human Upper Gastrointestinal Contents under Conditions Simulating Bioavailability/Bioequivalence Studies. *Pharm. Res.* **2006**, *23*, 165–176.
- Carriere, F.; Barrowman, J. A.; Verger, R.; Laugier, R. Secretion and Contribution to Lipolysis of Gastric and Pancreatic Lipases during a Test Meal in Humans. *Gastroenterology* **1993**, *105*, 876–888.
- Wickham, M.; Garrood, M.; Loney, J.; Wilson, P. D. G.; Fillery-Travis, A. Modification of a Phospholipid Stabilized Emulsion Interface by Bile Salt: Effect on Pancreatic Lipase Activity. *J. Lipid Res.* **1998**, *39*, 623–632.
- Hofmann, A. F. Bile Acids: The Good, the Bad, and the Ugly. *News Physiol. Sci.* **1999**, *14*, 24–29.
- Armand, M.; Borel, P.; Pasquier, B.; Dubois, C.; Senft, M.; Andre, M.; Peyrot, J.; Salducci, J.; Lairon, D. Physicochemical Characteristics of Emulsions during Fat Digestion in Human Stomach and Duodenum. *Am. J. Physiol.* **1996**, *271*, G172–G183.
- Staggers, J. E.; Hernell, O.; Stafford, R. J.; Carey, M. C. Physical-Chemical Behavior of Dietary and Biliary Lipids during Intestinal Digestion and Absorption. 1. Phase Behavior and Aggregation States of Model Lipid Systems Patterned after Aqueous Duodenal Contents of Healthy Adult Human Beings. *Biochemistry* **1990**, *29*, 2028–2040.
- MacGregor, K. J.; Embleton, J. K.; Lacy, J. E.; Perry, E. A.; Solomon, L. J.; Seager, H.; Pouton, C. W. Influence of Lipolysis on Drug Absorption from the Gastro-Intestinal Tract. *Adv. Drug Delivery Rev.* **1997**, *25*, 33–46.
- Mun, S.; Decker, E.; Park, Y.; Weiss, J.; McClements, D. Influence of Interfacial Composition on *in Vitro* Digestibility of Emulsified Lipids: Potential Mechanism for Chitosan's Ability to Inhibit Fat Digestion. *Food Biophys.* **2006**, *1*, 21–29.
- Troncoso, E.; Aguilera, J. M.; McClements, D. J. Influence of Particle Size on the *in Vitro* Digestibility of Protein-Coated Lipid Nanoparticles. *J. Colloid Interface Sci.* **2012**, *382*, 110–116.
- Qiu, H.; Caffrey, M. The Phase Diagram of the Monoolein/Water System: Metastability and Equilibrium Aspects. *Biomaterials* **2000**, *21*, 223–234.
- Salentinig, S.; Sagalowicz, L.; Glatter, O. Self-Assembled Structures and pK(a) Value of Oleic Acid in Systems of Biological Relevance. *Langmuir* **2010**, *26*, 11670–11679.
- Yaghmur, A.; de Campo, L.; Salentinig, S.; Sagalowicz, L.; Leser, M. E.; Glatter, O. Oil-Loaded Monolinolein-Based Particles with Confined Inverse Discontinuous Cubic Structure (Fd3m). *Langmuir* **2005**, *22*, 517–521.
- Israelachvili, J. N. *Intermolecular and Surface Forces*; Academic Press: Sydney, 1985.
- Hofmann, A. F.; Borgström, B. The Intraluminal Phase of Fat Digestion in Man: The Lipid Content of the Micellar and Oil Phases of Intestinal Content Obtained during Fat Digestion and Absorption. *J. Clin. Invest.* **1964**, *43*, 247–257.
- Hernell, O.; Staggers, J. E.; Carey, M. C. Physical-Chemical Behavior of Dietary and Biliary Lipids during Intestinal Digestion and Absorption. 2 Phase-Analysis and Aggregation States of Luminal Lipids during Duodenal Fat Digestion in Healthy Adult Human-Beings. *Biochemistry* **1990**, *29*, 2041–2056.
- Mazer, N. A.; Benedek, G. B.; Carey, M. C. Quasielastic Light-Scattering Studies of Aqueous Biliary Lipid Systems. Mixed Micelle Formation in Bile Salt-Lecithin Solutions. *Biochemistry* **1980**, *19*, 601–615.

32. Warren, D. B.; Anby, M. U.; Hawley, A.; Boyd, B. J. Real Time Evolution of Liquid Crystalline Nanostructure during the Digestion of Formulation Lipids Using Synchrotron Small-Angle X-Ray Scattering. *Langmuir* **2011**, *27*, 9528–9534.
33. Phan, S.; Hawley, A.; Mulet, X.; Waddington, L.; Prestidge, C.; Boyd, B. Structural Aspects of Digestion of Medium Chain Triglycerides Studied in Real Time Using sSAXS and Cryo-TEM. *Pharm. Res.* **2013**, *1–13*.
34. Fatouros, D. G.; Walrand, I.; Bergenstahl, B.; Müllertz, A. Colloidal Structures in Media Simulating Intestinal Fed State Conditions with and without Lipolysis Products. *Pharm. Res.* **2009**, *26*, 361–374.
35. Huang, T. C.; Toraya, H.; Blaton, T. N.; Wu, Y. X-Ray Powder Diffraction Analysis of Silver Behenate, a Possible Low-Angle Diffraction Standard. *J. Appl. Crystallogr.* **1993**, *26*, 180–184.
36. Yaghmur, A.; de Campo, L.; Sagalowicz, L.; Leser, M. E.; Glatter, O. Emulsified Microemulsions and Oil-Containing Liquid Crystalline Phases. *Langmuir* **2005**, *21*, 569–577.
37. de Campo, L.; Yaghmur, A.; Sagalowicz, L.; Leser, M. E.; Watzke, H.; Glatter, O. Reversible Phase Transitions in Emulsified Nanostructured Lipid Systems. *Langmuir* **2004**, *20*, 5254–5261.
38. Salonen, A.; Guillot, S.; Glatter, O. Determination of Water Content in Internally Self-Assembled Monoglyceride-Based Dispersions from the Bulk Phase. *Langmuir* **2007**, *23*, 9151–9154.
39. Levinger, N. E. Water in Confinement. *Science* **2002**, *298*, 1722–1723.
40. Sommer, A. P.; Zhu, D.; Foersterling, H. D.; Scharnweber, T.; Welle, A. Crystalline Water at Room Temperature - Under Water and in Air. *Cryst. Growth Des.* **2008**, *8*, 2620–2622.
41. Sommer, A. P.; Caron, A.; Fecho, H. J. Tuning Nanoscopic Water Layers on Hydrophobic and Hydrophilic Surfaces with Laser Light. *Langmuir* **2008**, *24*, 635–636.
42. Amar-Yuli, I.; Garti, N. Transitions Induced by Solubilized Fat into Reverse Hexagonal Mesophases. *Colloids Surf., B* **2005**, *43*, 72–82.
43. Phan, S.; Fong, W. K.; Kirby, N.; Hanley, T.; Boyd, B. J. Evaluating the Link between Self-Assembled Mesophase Structure and Drug Release. *Int. J. Pharm.* **2011**, *421*, 176–182.
44. Carey, M. C.; Small, D. M.; Bliss, C. M. Lipid Digestion and Absorption. *Annu. Rev. Physiol.* **1983**, *45*, 651–677.
45. Patton, J. S.; Carey, M. C. Watching Fat Digestion. The Formation of Visible Product Phases by Pancreatic Lipase is Described. *Science* **1979**, *204*, 145–148.
46. Nguyen, T.-H.; Hanley, T.; Porter, C. J. H.; Larson, I.; Boyd, B. J. Phytantriol and Glycerol Monooleate Cubic Liquid Crystalline Phases as Sustained-Release Oral Drug Delivery Systems for Poorly Water Soluble Drugs I. Phase Behaviour in Physiologically-Relevant Media. *J. Pharm. Pharmacol.* **2010**, *62*, 844–855.
47. Rizwan, S. B.; Boyd, B. J.; Rades, T.; Hook, S. Bicontinuous Cubic Liquid Crystals as Sustained Delivery Systems for Peptides and Proteins. *Expert Opin. Drug Delivery* **2010**, *7*, 1133–1144.
48. Tri-Hung, N.; Hanley, T.; Porter, C. J. H.; Boyd, B. J. Nanostructured Liquid Crystalline Particles Provide Long Duration Sustained-Release Effect for a Poorly Water Soluble Drug after Oral Administration. *J. Controlled Release* **2011**, *153*, 180–186.
49. Negrini, R.; Mezzenga, R. pH-Responsive Lyotropic Liquid Crystals for Controlled Drug Delivery. *Langmuir* **2011**, *27*, 5296–5303.
50. Negrini, R.; Mezzenga, R. Diffusion, Molecular Separation, and Drug Delivery from Lipid Mesophases with Tunable Water Channels. *Langmuir* **2012**, *28*, 16455–16462.
51. Chemelli, A.; Maurer, M.; Geier, R.; Glatter, O. Optimized Loading and Sustained Release of Hydrophilic Proteins from Internally Nanostructured Particles. *Langmuir* **2012**, *28*, 16788–16797.
52. Yaghmur, A.; Sartori, B.; Rappolt, M. The Role of Calcium in Membrane Condensation and Spontaneous Curvature Variations in Model Lipidic Systems. *Phys. Chem. Chem. Phys.* **2011**, *13*, 3115–3125.
53. Yaghmur, A.; Laggner, P.; Zhang, S.; Rappolt, M. Tuning Curvature and Stability of Monoolein Bilayers by Designer Lipid-Like Peptide Surfactants. *Plos One* **2007**, *2*, e479.
54. Barauskas, J.; Johnsson, M.; Tiberg, F. Self-Assembled Lipid Superstructures: Beyond Vesicles and Liposomes. *Nano Lett.* **2005**, *5*, 1615–1619.